Influence of end anchorage on shear strengthening of reinforced concrete beams using CFRP composites

Franklin F. R. Frederick*, U. K. Sharma and V. K. Gupta

Department of Civil Engineering, Indian Institute of Technology Roorkee, Roorkee 247 667, India

The article presents an experimental study on the influence of various end anchorage systems on the shear strengthening of reinforced concrete (RC) T-beams using externally bonded fibre reinforced polymer (EB-FRP) composites. Two different end anchorage techniques namely self-end anchorage (SEA) and sandwich anchorage (SWA) were used. This study mainly focussed on evaluating the effectiveness of these anchorages to eliminate the conventional fibre reinforced polymer (FRP) debonding failure. A total of twelve R.C. T-beams with different strengthening techniques using CFRP including control beams were used. The test results show improved shear strength and better energy dissipation over conventional technique; this authenticates the influence of end anchorage and its effectiveness in improving shear resistance. Also, the enhanced FRP strain at failure proves that the anchorage employed improves the efficacy of FRP strengthening in terms of ductility and damage tolerance.

Keywords: CFRP strengthening, external bonded FRP, end anchorage, shear behaviour.

MANY existing reinforced concrete (RC) structures in the world need reconstruction or strengthening because of ageing, lack of maintenance and up-gradation in code recommendations. Though conventional strengthening techniques such as RC jacketing, steel plate jacketing, ferrocement and fibre reinforced concrete strengthening[1–4] have been used, fibre reinforced polymer (FRP) wrapping has emerged as the most successful technique in recent years due to its ease and efficiency in construction practice. Strengthening of structural systems in India could be traced back from 1990s. Different types of fibre composites are available and the mechanical property of each material is unique as shown in Figure 1. Among the available fibre composites, GFRP and CFRP play a major role in strengthening with respect to their custom in industry. A single layer of CFRP can enhance the shear strength of a beam twice as compared with multiple layered GFRP composites as a result of its higher modulus. A review of FRP application in civil engineering[5] provides a detailed report on the strengthening works done in Indian railways using FRP such as Bata ROB–Kolkata (2005), Ghaghar Bridge (2005), Chandigarh Roon bridge (2006), and rehabilitation of a vertically cracked masonry bridge pier at Vijayawada–Visakhapatnam section of South Central Railway (2005).

A number of studies have been conducted on strengthening of RC elements using various FRP in the recent past[6–11]. The externally bonded FRP composites (EB-FRP) have been successfully used for upgrading the flexural, shear and axial load carrying capacities of RC elements. Many studies have focussed on the effect on shear strengthening of reinforced concrete (RC) elements[12–16]. Most of these studies[17–21] reported premature FRP debonding failure limiting the application of FRP on shear strengthening. In order to address this debonding failure many investigations have been done on different end anchorage systems using steel rod, steel plate and steel bolts as anchorage for FRP[22–26]. But these anchorage materials are prone to corrosion and not durable under severe environmental exposure conditions. It is understood from the literature that end anchorage technique improves the efficiency of FRP strengthening but requires a detailed study to investigate the effect of different end anchorage technique using FRP material. In this experimental study, two end anchorage systems are used and their influence studied in improving the shear resistance of RC beams.

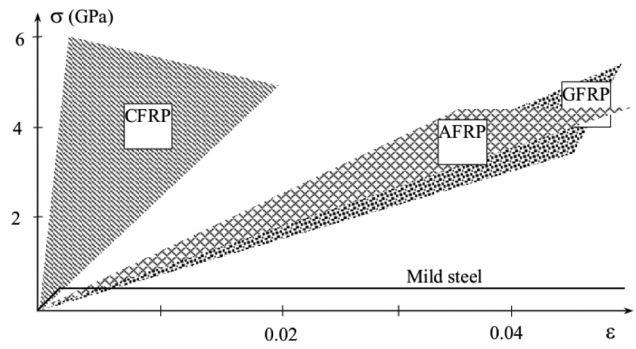

Figure 1. Uniaxial tension stress–strain diagrams for different unidirectional FRPs and steel[29].

*For correspondence. (e-mail: sheebu4174@yahoo.com)

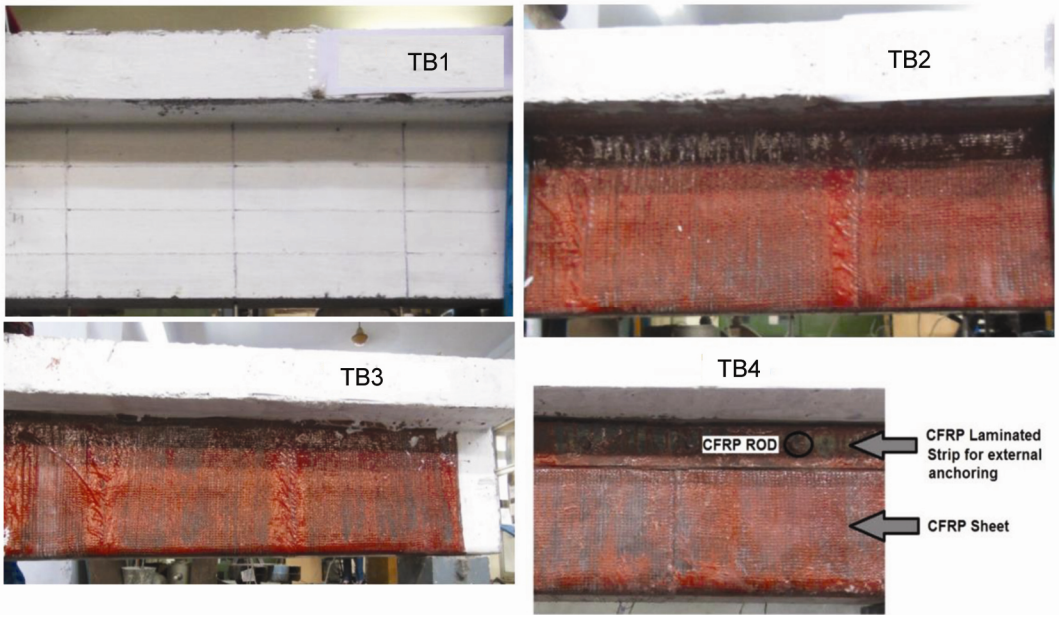

Figure 2. Detailed configuration of beam specimens.

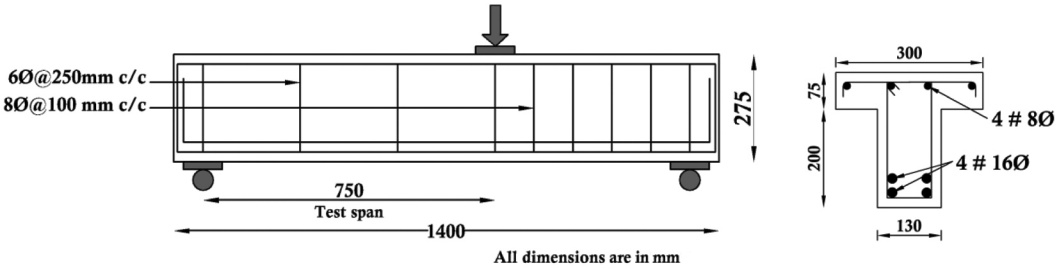

Figure 3. Beam specimen test setup and typical cross-section details.

Experimental programme

Three types of strengthening techniques using CFRP were employed in this study on strengthening of shear deficient R.C. T-beams with and without end-anchorage system. The longitudinal and transverse reinforcement ratio is kept the same in all beams to compare the performance of different strengthening techniques with conventional specimen. The conventional specimen is labelled as TB1, whereas the specimen strengthened with U-jacket EB-FRP method is labelled as TB2. The specimen with U-jacket EB-FRP and self end-anchorage (SEA) method is labelled as TB3 and the specimen strengthened with U-jacket EB-FRP and sandwich anchorage (SWA) method is labelled as TB4. Figure 2 shows the detailed strengthening schemes adopted in the study.

Details of R.C. T-beam specimens

The experimental programme consisted of R.C. T-beams with 1.4 m length. The cross-section and reinforcement details of test specimen are illustrated in Figure 3; it shows that the load point is located in the beam elevation so as to divide the effective length of the beam into a tested span (750 mm) on the left side and the shorter span (500 mm) on the right side. In test span 6 mm diameter steel stirrups were used at 250 mm pitch. The shorter span was confined with 8 mm diameter stirrups at 100 mm spacing to prevent any significant shear distress during testing, in order to avoid shear failure in the test span. The detailed configuration of test specimen is presented in Figure 3.

Materials specification

Ordinary Portland Cement (OPC-43 grade) and 12.5 mm downgraded coarse aggregates were used in concrete preparation with an average cube compressive strength of 34 MPa. Fe 500 grade steel for main reinforcement and Fe 415 for stirrups were used in this study. CFRP sheet of 0.15 mm thickness, CFRP fibre wrap sheet with an average tensile strength of 1400 MPa and 119 GPa tensile modulus; CFRP laminated strip with 50 mm width and

0.93 mm thickness with an average tensile strength of 1700 MPa and 196 GPa elastic modulus were used in strengthening works. Table 1 shows the properties (provided by the manufacturer) of CFRP.

Test set-up and instrumentation

All specimens were tested under three-point static loading with shear span-to-effective depth (a/d) ratio of 3.2. Test was carried out using 100 tonne hydraulic jack where the corresponding load and deflections were monitored using load cell and linear variable displacement transducers (LVDT). Strain gauges were placed on the side of beam web portion of CFRP in strengthened beams. Six strain gauges were installed on the CFRP sheet particularly in the shear-span region and oriented along the fibre direction of the section. The data from LVDT, strain gauges and load cell were scanned and recorded using a data acquisition system. The detailed load set-up and strain gauge positions are shown in Figure 4.

Strengthening method and practice

In strengthening work, surface of the strengthening zone was ground properly until the surface got dirt free, shown in Figure 5 *a*. Later a thin layer of primer coat was applied over the ground surface to fill voids and smoothen the surface (Figure 5 *b*). After 24 h, a layer of epoxy coating was applied over the primer coat (Figure 5 *c*). Finally the CFRP sheet was wrapped in U-shape over epoxy coating on the web portion of beam specimens (Figure 5 *d*). A fine roller was used to roll over the wrapped surface to remove the air voids. The above deliberated steps are common and followed in all strengthened beams. Typical details of strengthened specimen TB2 are shown in Figure 5 *f*. After surface grinding in specimen TB3, a groove was made with an average width of 5–7 mm and depth of 15–17 mm along two sides of the test span at the flange-to-web junction to provide self-end anchorage. Before wrapping, grooves were filled with epoxy simultaneously during epoxy coating on the surface. Later, the CFRP free end portions were inserted into the groove and of the test span at the flange-to-web junction. After FRP installation, grooves were filled with epoxy to fill the existing vacuum space inside as shown in Figure 6.

In specimen TB4, surface grinding was done initially and then horizontal holes with a diameter of 12 mm at 135 mm spacing were made perpendicular to the beam web surface. The distance between the centres of the hole to the beam flange was kept as 35 mm. Before wrapping, CFRP rods were coated with adhesive for better anchorage. During CFRP wrapping, the free end of CFRP was rolled with a 50 mm width CFRP laminated strip. This laminated strip has predrilled holes, once the wrapping work was completed the adhesive coated CFRP rods were inserted into the holes through laminated strip holes as shown in Figure 7 *c*. The detailed step-by-step procedure of sandwich anchorage method is illustrated in Figure 7. Figure 7 *e* shows the typical details of specimen TB4.

Table 1. Properties of carbon fibre wrap and laminate

Typical fibre properties	Units	CFRP fibre wrap	CFRP laminated strip
Tensile strength	MPa	1400	1,700
Tensile modulus	GPa	119	196
Density	g/cm^3	1.6	1.7
Ultimate elongation	%	–	0.707

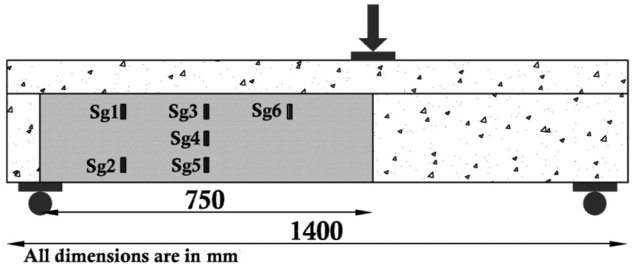

Figure 4. Location of strain gauges on specimen.

Results and discussion

RC T-beams with different configuration were cast and tested under static loading to examine the effect of additional anchorage in shear performance of the specimens. The details of test results are discussed in the following section.

Failure analysis

All beam specimens exhibit different failure modes with respect to the configuration. Figure 8 shows failure pattern of all tested specimens. In control beam (TB1), initially vertical cracks occurred and as the load increases those vertical cracks turned inclined. During further loading, shear cracks started to spread across the span both in confined and unconfined zones. The inadequate confinement in the unconfined zone led the specimen to fail in brittle mode as shown in Figure 8 *a*. In beam (TB2) with external CFRP wrapping without anchorage, inclined cracks were noticed at confined zone up to a threshold, later inclined cracks were observed in the web region of unconfined zone and popping sound were also heard as evidence of cracking in the strengthened region. As a result of CFRP delamination, the specimen lost its resistance to shear force after yielding. Delamination occurred in the place where TB1 exhibits failure with primary shear cracks as depicted in Figure 8 *b*.

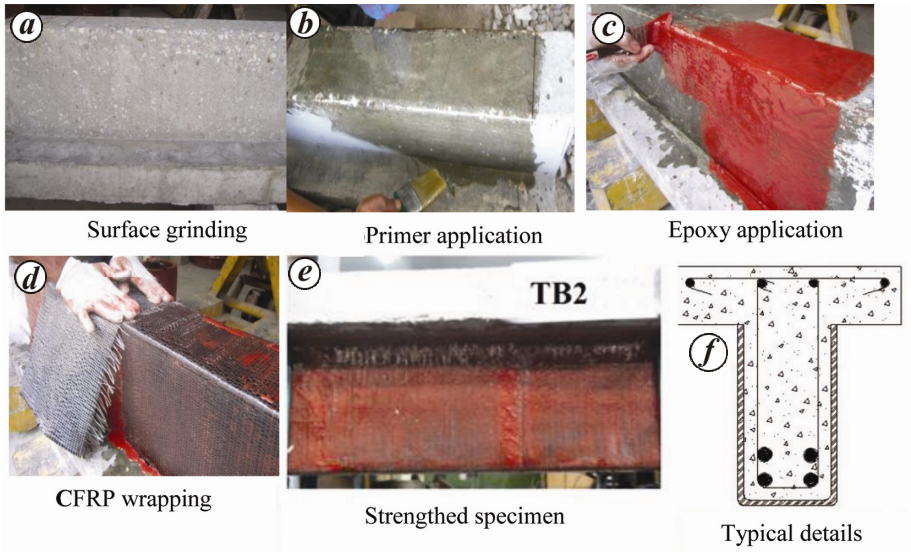

Figure 5. Detailed procedure of specimen TB2 strengthening technique.

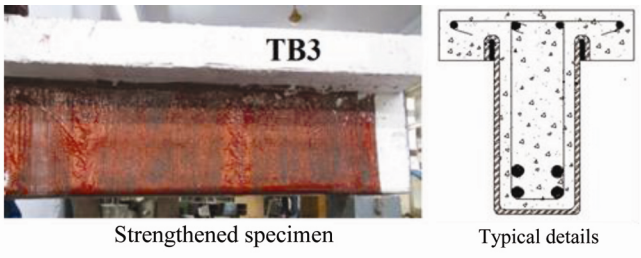

Figure 6. Details of specimen TB3.

The specimen TB3 with SEA technique resisted shear force and transferred the applied force across the span effectively. As a result of this anchorage, flexural cracks started becoming wide enhancing the post-yield deflection behaviour of the specimen. Whereas in TB1 and TB2 shear cracks were noticed in the confined zone, the crack width in the unconfined zone led the specimen to fail immediately after yield. In TB3 there was no inclined crack in the web portion of the unconfined zone. After certain deflection, popping sound was heard in the strengthened zone and finally FRP unzipped vertically as depicted in Figure 8 *c*. Failure pattern of TB3 emphasized the importance of anchorage in FRP strengthening technique over conventional technique.

In the specimen (TB4) with SWA technique, the failure pattern was entirely different as compared to SEA technique. Numerous inclined cracks were noticed in the confined zone. Unlike TB3, it shows a gradual deflection pattern like a beam with adequate confinement. In specimen TB3 flexural cracks in the confined zone allowed the specimen to deflect whereas in TB4, cracks were initiated in the strengthened zone and as the deflection increased the CFRP unzipped vertically in numerous places allowing the beam to deflect uniformly to attain higher deflection than all other specimens. During large deflection the anchored region pulled it off and the bottom surface of CFRP was ruptured as shown in Figure 8 *d*. This confirms that the failure pattern and performance enhancement depends on the anchoring method.

Load-deflection behaviour

The load-deflection behaviour of tested specimens is shown in Figure 9 and the test results are summarized in Table 2. The load-deflection curve shows that the strengthened beams have better initial stiffness over TB1. This is due to the initial resistance to deflection because of the employed CFRP wrapping. While considering load deflection curve, TB1 is linear up to 200 kN whereas in other strengthened specimen the linearity is observed up to 350 kN. The post-yield deflection behaviour of specimens TB1 and TB2 shows sudden brittle failure; though the beam is strengthened with CFRP (TB2) wrapping the specimen failed to resist the load at higher deflection. Due to the absence of FRP anchorage, debonding occurs at a premature stage and finally exhibits brittle failure.

The load-deflection curve of specimen TB3 shows the effectiveness of anchorage in strengthening scheme and emphasized the importance of anchorage. In FRP strengthening technique, the strength enhancement of a particular structural member is predominant rather than ductility. Thus, FRP can withstand up to a certain load. When a load higher than the design load is applied, debonding will occur and will lead the specimen to fail in brittle mode. In order to effectually utilize the strengthening technique proper anchorage is advisable. This SEA mechanism confines the shear deficient zone effectively and allows the confined zone to deflect more as the load increases. Thus the specimen attains 100% higher deflection

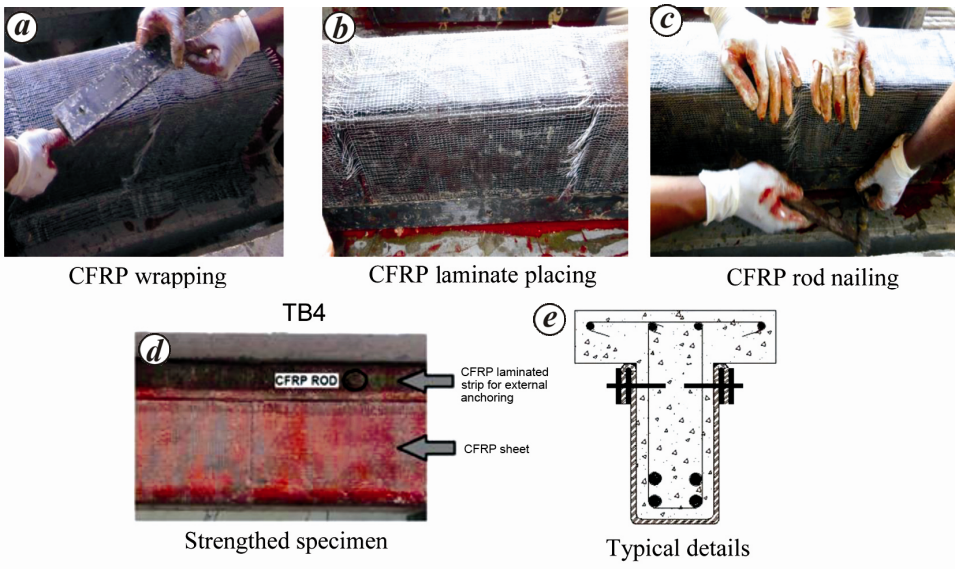

Figure 7. Detailed procedure of specimen TB4 strengthening technique.

behaviour with 48% higher shear resistance capacity than TB1 and TB2. As deflection increases, the CFRP unzipped vertically rather than debonding. Thus SEA technique experiences better post-yield response over TB2.

Strength and stiffness degradation

Stiffness of a structural element is a measure of resistance to deformation. The difference between yield stiffness and secant stiffness demonstrates the inelastic behaviour of a structural component[27]. The post-elastic strength degradation over yield strength and post-elastic stiffness degradation over yield stiffness are calculated to estimate the inelastic behaviour of all beam specimens. The rate of change in strength and stiffness degradation over post-elastic rotation define the inelastic performance of beam specimens. Higher rate of degradation shows brittle response of structural component with vice versa. Figure 10 shows the stiffness and strength degradation of all beam specimens.

Figure 10 shows sudden rate of increase in strength and stiffness degradation at 0.005 rad in TB1 and TB2, possibly because of brittle failure. This failure significantly affects the stiffness retention capacity. Figure 10 validates the importance of FRP anchorage in strengthening work, both the specimens TB3 and TB4 demonstrate 100% higher stiffness retention over TB1 and TB2. At 0.005 radian TB3 and TB 4 show 40% stiffness degradation and at 0.0175 rad it is 70% degradation. This rotation difference authenticates the activeness of the employed SEA and SWA technique on stiffness retention in post-yield region. Both TB1 and TB2 experienced sudden drop in strength at 0.005 rad but the specimens with additional anchorage TB3 and TB4 show steady state of strength after 0.005 rad up to 0.0175 rad. The inelastic behaviour and stiffness degradation behaviour of TB4 show the uniqueness of end-anchorage system in strengthening technique. Stiffness degradation behaviour of specimen TB4 is nearly equal to the specimen TB3 up to a threshold; later due to vertical cracks in FRP the rate of degradation increases a little higher in specimen TB4 than TB3 (Figure 10). It can be concluded that the specimen with additional end-anchorage enhances the post-yield response and increases the stiffness retention capacity over other strengthened beam without anchorage.

Effect of anchorage on shear strength

Figure 11 shows 15% shear capacity gains in EB-strengthened specimen with no end-anchorage as compared to control beam TB1. Beam TB3 which was strengthened with self-end anchorage shows 48% higher shear carrying capacity than the control beam. In addition, Figure 11 shows that the beam TB4 experiences 29% higher shear carrying capacity than the control beam. Beams strengthened using EB-FRP SEA system and double–CFRP laminated plate SWA system show highest shear capacity gain compared to the EB-FRP system. RC T-beams TB3 and TB4 reached 29% and 12% higher shear capacity compared to EB-FRP system. This authenticates the efficacy of the synergetic effect of end-anchorage and FRP strengthening in improving the shear carrying capacity of the beam.

Effect of anchorage on ductility

In order to examine the effect of strengthening technique employed on ductile behaviour, displacement ductility and energy dissipation were calculated (Figure 12). Ductility (μ) is the ability of deformation beyond initial yield deformation without significant loss in strength. Ductility

Table 2. Summarized test results of all beam specimens

Specimen ID	Load at rupture (kN)	Total shear resistance (kN)	Resistance due to CFRP (kN)	Gain due to CFRP (%)	Gain due to anchorage (%)	Deflection (mm)	Ductility (μ)	Failure mode
TB1	305	122.0	–	–	–	6.4	2	Shear
TB2	350	140.0	18.0	15	–	6.0	2.14	Shear
TB3	452	180.8	58.8	48	29	15.0	3.75	Flexure
TB4	392	156.8	34.8	29	12	13.5	3.29	Shear

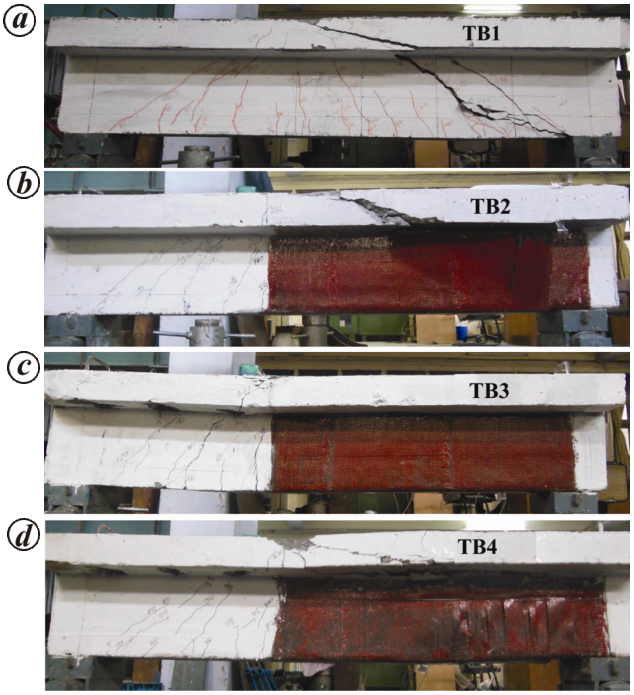

Figure 8. Failure pattern of tested beam specimen.

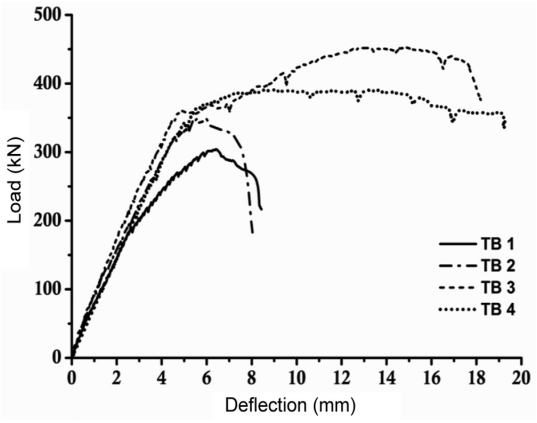

Figure 9. Load–deflection curves of RC T-beams.

factor (μ)[27] is defined as the ratio of ultimate deflection (Δ_u) to yield deflection (Δ_y), eq. (1) and the measured ductility is presented in Table 2. The ductility performance of a structural component entirely depends on its post-yield response and the dissipated energy level during loading. The sudden shear failure in control specimen

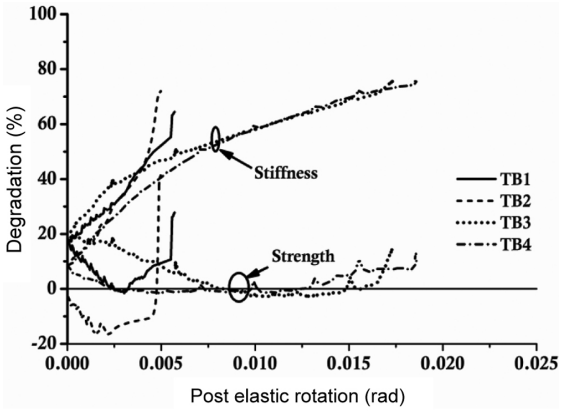

Figure 10. Strength and stiffness degradation plot.

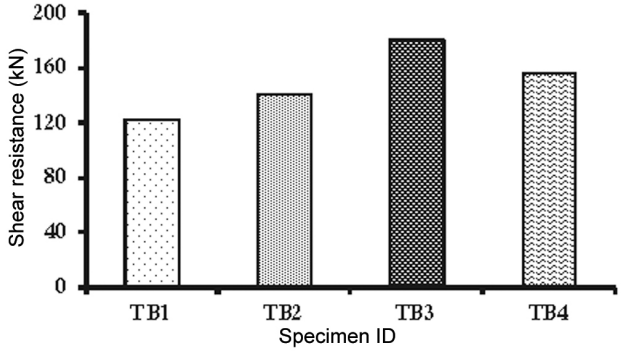

Figure 11. Shear resistance of RC T-beams.

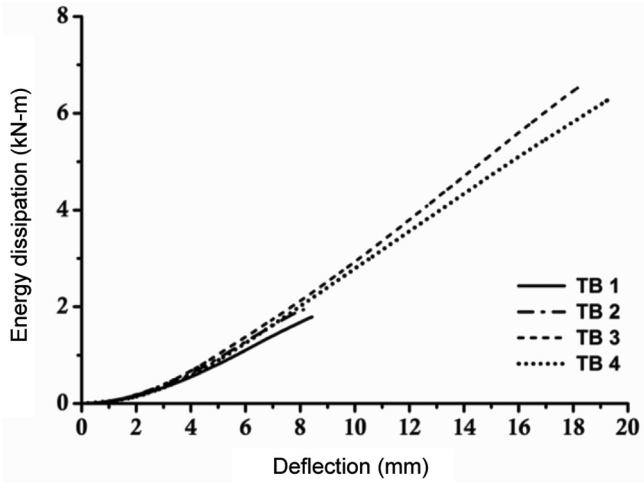

Figure 12. Cumulative energy dissipation.

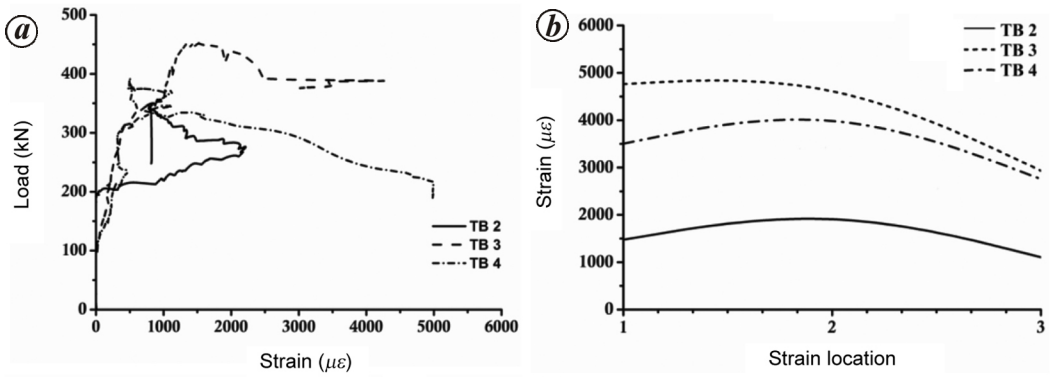

Figure 13. Load versus maximum strain in CFRP.

Table 3. Efficiency of the anchorage method

Specimen ID	Area of dry fibre (mm^2/m)	Ultimate tensile capacity per unit length (kN/m)	V_f (kN)	Efficiency of FRP ψ_f (% m)
TB2	450	630	18.0	2.85
TB3	450	630	58.8	9.33
TB4	450	630	34.8	5.52

Table 4. Comparison between measured and calculated CFRP strains

Specimen ID	Experimental maximum measured CFRP strain ($\mu\varepsilon$)	ACI 440.2R-08 calculated CFRP strain ($\mu\varepsilon$)
TB1	–	–
TB2	2215	3434
TB3	4409	3434
TB4	4992	3434

shows poor ductile behaviour as compared to other specimens. The specimen TB2 does not exhibit better post-yield behaviour. But the premature FRP debonding failure in specimen TB2 restricts the energy dissipation as compared to other specimens with anchored strengthening technique. The specimen with SEA shows better post-yield behaviour than TB1 and TB2 specimens. This enhanced inelastic response allows the specimen TB3 to dissipate 130% higher energy and shows more than 60% increase in ductility than the specimen without end-anchorage. It emphasized the importance and effectiveness of end-anchorage system on energy dissipation. The specimen with SWA technique demonstrates the efficiency of this anchorage technique in ductility enhancement and energy dissipation over other methods. The measured ductility factor and energy dissipation of anchorage enabled specimens prove the necessity of additional end anchorage in performance enhancement over TB1 and TB2 specimens respectively. The difference in ductility property is negligible for specimens TB3 and TB4, thus it can be concluded that both SWA and SEA techniques play an effective role in resisting shear force with enhanced post-peak deflection behaviour without sudden loss in strength.

$$\mu = \frac{\Delta_u}{\Delta_y}. \quad (1)$$

Efficiency of the anchorage method

To quantify the effectiveness of the anchorage technique employed with EB-FRP method on shear strengthening, an efficiency measure was assessed and compared with the performance of EB-FRP method without end-anchorage. The efficiency of FRP strengthening is defined as the ratio between shear strength contributions of CFRP (v_f) to the CFRP ultimate tensile capacity per unit length. The calculated efficiency level of all the FRP strengthening methods is presented in Table 3. The specimen TB2 without anchorage shows meagre efficiency level as compared to anchored specimen. The specimen with anchorage (TB3) exhibits an average of 90–200% higher efficiency level over EB-FRP without anchorage system. The observed difference in efficiency level between specimens TB3 and TB4 shows 50% higher efficiency level in SEA method over SWA method. This is possibly because the SEA technique employed helps the specimen to withstand higher load with better post-yield behaviour.

However, with higher ductility, the FRP unzipping phenomena limit the efficiency level of beam strengthened with sandwich anchorage method.

Debonding strain

The effective strain is the maximum strain that can be achieved in the FRP system at the nominal strength which is governed by the failure mode of the FRP system. According to the required configuration, strengthening method should be preferred. The method of selection is based on possible failure modes and effective strain observed from the research work. Higher FRP strain shows the enhanced effectiveness of strengthening scheme. A professional could choose a FRP strengthening technique and the type of FRP based on the effective strain and its failure mode. The observed effective strain of all test specimens provide regulation on defining this effective strain for different anchorage configurations of FRP wrapping used for shear strengthening of the reinforced concrete beam.

Figure 13 shows load versus maximum CFRP strain response of all strengthened specimens. It shows that at initial stage there is no strain increment in CFRP sheets and the strain curves of all strengthened beams remain the same up to 125 kN. Strain increase is observed in CFRP sheets after the applied load reaches approximately 125–200 kN. Upon load increase, the strain level also increases at a relatively higher rate until failure. Strain level differs according to the adopted strengthening technique. In specimen TB2, strain level increased after 150 kN and at peak load the strain is 2215 $\mu\varepsilon$. When the load level reached 267 kN some popup noise is heard and the CFRP start to debond from the concrete substrate due to inadequate anchorage and restricts strain increase.

The failure pattern and strain values of specimen TB3 differ from TB2. Figure 13 *a* shows that the strain at maximum load is 1415 $\mu\varepsilon$; during post-peak loading the strain value increases to a new high level (4409 $\mu\varepsilon$) because of the employed additional end-anchorage. This SEA holds the CFRP to stick with concrete substrate and eliminates the premature FRP debonding. The observed strain in TB3 is 49% higher than TB2 specimen. The strain behaviour of specimen strengthened with SWA differs from other methods. The observed strain value of 510 $\mu\varepsilon$ at a maximum load 392 kN shows that the provided anchorage restricts the FRP strain at initial stage. At failure, the strain value of 4492 $\mu\varepsilon$ in TB4 reveals that it is significantly higher than all other specimens including specimen with SEA. Overall, the strengthened specimens with adequate anchorage show higher strain because of the absence of premature FRP debonding.

ACI 440-2008 provides the calculation method to estimate the effective strain of U-wrapped CFRP sheet without end-anchorage using following equations

$$\varepsilon_{fe} = K_v \varepsilon_{fu} \le 0.004, \tag{2}$$

where ε_{fe} is the effective strain in CFRP sheet, K_v the coefficient to calculate the effective CFRP strain, ε_{fu} is the ultimate strain of CFRP

$$\kappa_v = \frac{\kappa_1 \kappa_2 L_e}{11{,}900\varepsilon_{fu}} \le 0.75, \tag{3}$$

where κ_1, κ_2 are the modification factors applied to κ_v to account for concrete strength, and wrapping scheme respectively, L_e is the active bond length of CFRP.

$$L_e = \frac{23{,}300}{(n_f t_f E_f)^{0.58}}, \tag{4}$$

where n_f is the number of CFRP layers, t_f the thickness of one layer of CFRP, E_f is the Young's modulus of CFRP

$$\kappa_1 = \left(\frac{f_c'}{27}\right)^{2/3}, \tag{5}$$

where f_c' is the compressive strength of concrete

$$\kappa_2 = \frac{d_{fv} - L_e}{d_{fv}}. \tag{6}$$

where d_{fv} is the effective depth of CFRP shear reinforcement.

The effective strain in U-shaped CFRP sheets can be estimated using eqs (2)–(6). A comparison between the maximum measured CFRP strains and the calculated values on the basis of the ACI-440-2008 (ref. 28) formula is presented in Table 4. The code estimates the FRP strain without anchorage; hence the calculated strain value for specimen without anchorage is used to quantify the increase in strain due to the additional anchorage. The increase in strain due to the employed anchorage technique can be understood from Table 4. It shows that ACI-440-2008 (ref. 28) overestimates the CFRP strain without anchorage. The strain increase due to anchorage shows that the code underestimates the strain capacity.

Conclusions

The aim of this study was to evaluate the effect of end-anchorage on shear strengthening of RC beams using EB-FRP methods. The following conclusions are drawn on the basis of experimental results.

(1) EB-FRP with SEA system can significantly improve the shear resistance capacity of RC beams with better post-yield behaviour. An average of 48% higher shear

resistance capacity and two-fold higher post yield deflection are observed in the beam strengthened using EB-FRP with SEA as compared to the strengthened beam without anchorage.

(2) Beam strengthened using EB-FRP with SWA also enhances the post-yield behaviour and shear resistance capacity. An average of 200% higher post-yield defection than the strengthened specimen without anchorage is observed. The difference in shear resistance capacity is very minor but the beam sustained the load up to failure. This observed post-yield deflection emphasizes the effectiveness of the SWA technique in EB-FRP method.

(3) All the strengthened beams exhibit higher stiffness but the strengthened beam with end-anchorage shows better stiffness retention and gradual stiffness degradation during inelastic loading as compared to the specimen without anchorage.

(4) The use of SEA system enhances the energy dissipation capacity and ductility by holding the post-yield load carrying capacity to better deflection. An average of two-fold higher energy dissipation and ductility behaviour is observed in beam with end-anchorage over beam without anchorage.

(5) The absence of end-anchorage in TB2 leads the specimen to fail in debonding failure. However, the EB-FRP with adequate anchorage does not fail because of debonding and alters the failure mode to brittle shear.

(6) The observed FRP strain and efficiency level emphasize the importance of adequate anchorage in the EB-FRP strengthening technique. The observed strain at failure is nearly 200% higher than the strengthened beam without end-anchorage.

1. Fatih, A., An experimental study of the jacketed reinforced-concrete beams under bending. *Constr. Build Mater*., 2004, **18**, 611–618.
2. Adhikary, B. B. and Mutsuyoshi, H., Shear strengthening of RC beams with web-bonded continuous steel plates. *Constr. Build Mater*., 2004, **20**, 296–307.
3. Giovanni, M., Alberto, M., Giovanni, A. and Zila, R., Strengthening and repair of RC beams with fibre reinforced concrete. *Cem. Conc. Comp*., 2010, **32**, 731–739.
4. Paramasivam, P., Lim, C. T. E. and Ong, K. C. G., Strengthening of RC beams with ferrocement laminates. *Cem. Conc. Comp.*, 1998, **20**, 53–65.
5. Shrivastava, R., Gupta, U. and Choubey, U. B., FRP: research, education and application in India and China in civil engineering. *Int. J. Rec. Tren. Eng*., 2009, **1**(6), 89–93.
6. Barros, J. A. O., Dias, S. J. E. and Lima, J. L. T., Efficacy of CFRP-based techniques for the flexural and shear strengthening of concrete beams. *Cem. Con. Comp.*, 2007, **29**, 203–217.
7. Taljsten, B., Strengthening concrete beams for shear with CFRP sheets. *Constr. Build Mat.*, 2003, **17**, 15–26.
8. Abdelhak, B. and Omar, C., Behaviour of reinforced concrete T-beams strengthened in shear with carbon fibre-reinforced polymer – an experimental study. *ACI Struct. J.*, 2006, **103**, 3.
9. Chaallal, O., Shahawy, M. and Hussan, M., Performance of reinforced concrete T-girders strengthened in shear with carbon fibre-reinforced polymer fabric. *ACI Struct. J.*, 2002, **99**(3), 335–343.
10. Al-Amery, R. and Al-Mahaidi, R., Coupled flexural-shear retrofitting of RC beams using CFRP straps. *Composite Struct.*, 2006, **75**(1–4), 457–464.
11. Bencardino, F., Spadea, G. and Swamy, R. N., Strength and ductility of reinforced concrete beams externally reinforced with carbon fibre fabric. *ACI Struct. J.*, 2002, **99**(2), 163–171.
12. Sundarraja, M. C. and Rajamohan, S., Strengthening of RC beams in shear using GFRP inclined strips – an experimental study. *Constr. Build Mat*., 2009, **23**, 856–864.
13. Grace, N. F., Sayed, G. A., Soliman, A. K. and Saleh, K. R., Strengthening reinforced concrete beams using fibre reinforced polymer (FRP) laminate. *ACI Struct. J.*, 1999, **96**(5), 865–874.
14. Saadatmanesh, H. and Tannous, F. E., Long term behaviour of aramid fibre reinforced plastic (AFRP) tendons. *ACI Mater. J.*, 1999, **96**(3), 297–305.
15. Chaallal, O., Mofidi, A., Benmokrane, B. and Neale, K., Embedded through-section FRP rod method for shear strengthening of RC beams: performance and comparison with existing techniques. *J. Comp. Constr.*, 2011, **15**(3).
16. Khalifa, A. and Nanni, A., Rehabilitation of rectangular simply supported RC beams with shear deficiencies using CFRP composites. *Constr. Build Mater*., 2002, **16**, 135–146.
17. Ting, J. G., Smith, S, T., Yao, J. and Chen, J. F., Intermediate crack-induced debonding in RC beams and slabs. *Constr. Build Mater*., 2003, **17**(6–7), 447–462.
18. Smith, S. T. and Ting, J. G., FRP-strengthened RC beams. I: review of debonding strength models. *Eng. Struct.*, 2002, **24**, 385–395.
19. Ozgur, A., Strengthening of RC T-section beams with low strength concrete using CFRP composites subjected to cyclic load. *Constr. Build Mater*., 2008, **22**, 2355–2368.
20. Khalifa, A. and Nanni, A., Improving shear capacity of existing RC T-section beams using CFRP composites. *Cem. Con. Comp.*, 2000, **2**, 165–174.
21. Zhichao, Z., Cheng-Tzu and Thomas Hsu, Shear strengthening of reinforced concrete beams using carbon–fibre–reinforced polymer laminates. *J. Comp. Constr.*, 2005, **9**(2).
22. Adhikary, B., Mutsuyoshi, H. and Ashrof, M., Shear strengthening of reinforced concrete beams using fibre reinforced polymer sheets with bonded anchorage. *ACI Struct. J.*, 2004, **101**(5), 660–668.
23. Khaled, G. and Amir, M., Shear strengthening of RC T-beams using mechanically anchored unbonded dry carbon fibre sheets. *J. Per. Const. Facs*, 2010, **24**(1), 31–39.
24. Franklin, F. R. F., Sharma, U. K. and Gupta, V. K., Shear behaviour of externally confined R.C beams using CFRP with end anchorage. In Proceedings of the Sixth International Conference Asian. Conc. Fed., September, Seoul, Korea, 2014.
25. Chen, J. F. and Ting, J. G., Anchorage strength models for FRP and steel plates bonded to concrete. *J. Struct. Eng.*, 2001, **127**(7), 784–791.
26. Abdeldjelil, B. and Sang, W. B., Antonio Brancaccio. Behavior of full-scale RC T-beams strengthened in shear with externally bonded FRP sheets. *Const. Build. Mater*., 2012, **32**, 27–40.
27. Siva Chidambaram, R. and Pankaj Agarwal, Flexural and shear behaviour of geo-grid confined RC beams with steel fibre reinforced concrete. *Const. Build. Mat.*, 2015, **78**, 271–280.
28. ACI 440.2R-08. Guide for the design and construction of externally bonded FRP systems for strengthening concrete structures. 2008.
29. The International Federation for Structural Concrete (CEB-FIB), Technical Report Bulletin 14. Externally bonded FRP reinforcement for RC structures, 2002.

Received 20 February 2016; revised accepted 21 September 2016

doi: 10.18520/cs/v112/i05/973-981